$E1$ and $M1$ γ-strength functions in ^{144}Nd

A. V. Voinov* and S. M. Grimes
Department of Physics and Astronomy, Ohio University, Athens, Ohio 45701, USA
(Received 12 August 2015; published 14 December 2015)

Both $E1$ and $M1$ γ-strength functions below the neutron separation energy were analyzed based on experimental data from ^{143}Nd(n,γ) ^{144}Nd and ^{143}Nd$(n,\gamma\alpha)$ ^{140}Ce reactions. It is confirmed that the commonly adopted $E1$ model based on the temperature dependence of the width of the giant dipole resonance works well. The popular $M1$ strength function due to the spin-flip magnetic resonance located near the neutron binding energy is not capable of reproducing experimental data. The low-energy enhancement of the $M1$ strength or the energy-independent model of Weisskopf, both leading to the low-energy strength sizable to $E1$ one, fit experimental data best.

DOI: 10.1103/PhysRevC.92.064308 PACS number(s): 21.10.Ma, 21.10.Pc, 24.60.Dr, 28.20.Np

I. INTRODUCTION

The experimental study of low-energy (1–3 MeV) γ transitions between highly excited compound states in the continuum populated in nuclear reactions has always been a challenging problem. The nature of the strength of such transitions is still poorly understood. This is related largely to experimental difficulties of isolating such transitions from the usually more-intense, same-energy transitions between low-lying discrete nuclear levels in experimental γ spectra.

The first experimental estimation of the strength of such transitions has been done with the ^{143}Nd$(n^{\text{th}},\gamma\alpha)^{140}$Ce reaction where the compound nucleus ^{144}Nd formed with the thermal-neutron-capture reaction decays down by the cascades consisting of the primary low-energy γ and the secondary α transitions. Several such experiments have been performed with consistent results [1–3]. The $\gamma\alpha$ cascades are seen as a continuum distribution in the α spectrum between peaks corresponding to population of the ground state and the 1.5 MeV 2^+ first-excited state of ^{140}Ce (Fig. 1). The shape of this distribution was used to determine the γ strength for low-energy γ transitions between excited compound states. Specifically, it was found that the hypothesis of a zero low energy $E1$ strength function limit ($f_{E1}(E_\gamma)_{E_\gamma\to 0}$) resulted from extrapolation of the giant dipole resonance with the Lorentz function is not correct. The new model was developed for the $E1$ strength assuming its dependence on the temperature of final states [4]. Since then similar models have been proposed for the $E1$ strength function [5]. All these models are now used in nuclear reaction codes [6,7]. The general feature of all $E1$ strength function models is the nonzero limit of $E1$ strength [$f_{E1}(E_\gamma)_{E_\gamma\to 0} \to \sim 10^{-8}$ MeV^{-3}]. Such a limit results from the spreading of the giant dipole resonance (GDR) width which is due to its dependence on both the γ energy and the temperature of final states populated by γ transitions [4].

However, the following assumptions were made when the analysis of the $(n,\gamma\alpha)$ reaction was performed [3]. The effect of the level density on shape of the $\gamma\alpha$ spectrum was assumed to be negligible. The strength of low-energy $M1$ transitions, which were postulated to play an important role, was approximated by the Weisskopf single-particle model [8] which assumes an independence of the γ strength on the γ energy, i.e., $f_{M1}(E_\gamma) = \text{const}$. However, as is shown later [5], the γ spectra and total radiative widths of neutron resonances for spherical nuclei from the same mass range are reproduced best with the assumption of $M1$ strength based on the Lorentzian function (not Weisskopf estimate). The latter model is based on the spin-flip $M1$ giant resonance, which predicts the $M1$ strength to be about 100 times less than either the $E1$ or the Weisskopf $M1$ ones for low-energy γ transitions that is not in accord with the conclusion from the $(n,\gamma\alpha)$ analysis [9]. Now, modern reaction codes, such as EMPIRE [6] and TALYS [7] use RIPL-3 database recommendations for the $M1$ strength function which is assumed to be due to an $M1$ spin-flip resonance described by the Lorentzian function centered around the neutron separation energy [10]. On the other hand, there are results seen from Oslo-type experiments indicating the low-energy enhancement of the γ-strength function in different mass regions, which was interpreted as an enhancement of the $M1$ strength [11].

In order to resolve the existing ambiguities about the $M1$ strength function, it appears to be important to reanalyze the data from the ^{143}Nd$(n,\gamma\alpha)$ reaction taking into account new developments and new experimental data that have been obtained after the publication of Ref. [4].

II. METHOD OF ANALYSIS

In the statistical reaction model the cross section of the $(n,\gamma\alpha)$ reaction proceeding through the initial i, intermediate j, and final f states can be expressed in the following manner:

$$\overline{\frac{d\sigma}{dE_\alpha}}(E_\alpha) = \overline{\sigma}_i \frac{\sum_{XLL'} \overline{\Gamma}_{ij}^{XL}(E_\gamma)\overline{\Gamma}_{jf}^{L'}(E_\alpha)}{\overline{\Gamma}_i(B_n)\overline{\Gamma}_j(B_n - E_\gamma)} \rho^j(B_n - E_\gamma), \quad (1)$$

where $\overline{\sigma}_i$ is the capture-cross-section average over resonances with the same spin and parity, $\overline{\Gamma}_{ij}(E_\gamma)$ is the average width of the primary γ transition, $\overline{\Gamma}_i(B_n)$ is the total average γ width of the initial i compound state, $\overline{\Gamma}_j(B_n - E_\gamma)$ is the total average width of the intermediate j level populated by the primary γ transition E_γ, $\overline{\Gamma}_{jf}(E_\alpha)$ is the average α width of the

*voinov@ohio.edu

 ©2015 American Physical Society

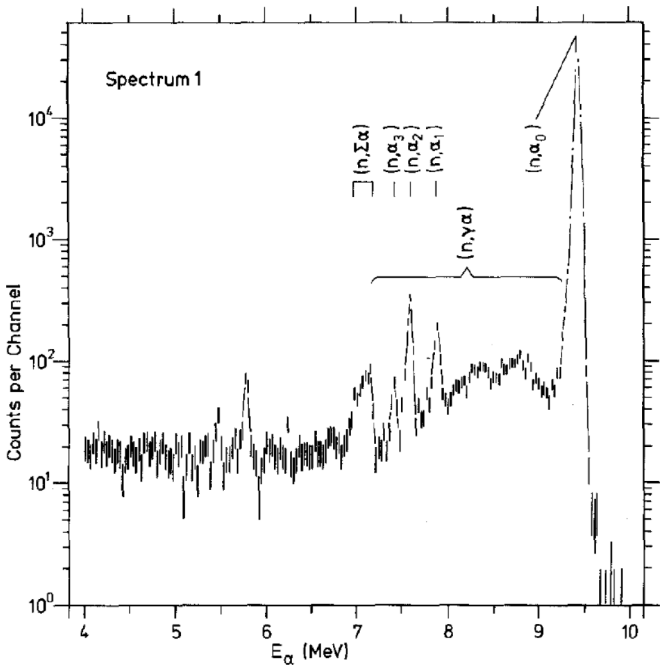

FIG. 1. α spectrum from thermal neutron capture reaction on ^{143}Nd. The figure is taken from Ref. [2] (Fig. 1), with permission from Springer.

intermediate level j decaying to the final level f. $\rho^j(B_n - E_\gamma)$ is the density of intermediate levels j. Here we assume that a compound nucleus is formed with the excitation energy equal to the neutron separation energy B_n. The summation is performed over all possible multipolarities XL of γ transitions and orbital momenta L' of α particles. The γ and α widths are expressed in terms of the γ-strength function $f_{XL}(E_\gamma)$ and α-transmission coefficients $T^{L'}(E_\alpha)$, respectively, as

$$\overline{\Gamma}_{ij}^{XL}(E_\gamma) = \overline{D_i} E^{2l+1} f_{Xl}(E_\gamma), \tag{2}$$

$$\overline{\Gamma}_{jf}^{L'}(E_\alpha) = \frac{T^{L'}(E_\alpha)}{2\pi}\overline{D_j}, \tag{3}$$

where $\overline{D_i}$ and $\overline{D_j}$ are average spacings of i and j levels, respectively. The α-transmission coefficients are calculated from optical model potentials. One can see that, in order to estimate the γ-strength function from Eqs. (1)–(3), the $\overline{\Gamma}_{jf}^{L'}(E_\alpha)$ functions must be known. However, the α-optical potentials for α energies 7–9 MeV, which is way below the Coulomb barrier, are highly uncertain. Potentials collected in the RIPL-3 database [10] produce transmission coefficients which differ up to 20 times from each other in this energy range. Therefore, first, we tested α-optical potentials against experimental data on the ^{143}Nd(n,α) reaction. Cross sections for 2 to 500 keV neutrons have been measured recently in Ref. [12]. At these energies Porter–Thomas fluctuations of individual resonances can be neglected so the measured cross sections are the ones averaged over resonances. The ^{143}Nd(n,γ) cross sections were measured in Ref. [13] for the same neutron energies. Taking into account that the ratio of total (integrated over energies of an outgoing particle or γ) cross sections is proportional to the ratio of total widths, $\overline{\sigma}_{n,\alpha}/\overline{\sigma}_{n,\gamma} \propto \overline{\Gamma}_\alpha/\overline{\Gamma}_\gamma$, and the experimental $\overline{\Gamma}_\gamma^{\rm expt} = 73$ meV [14], the $\overline{\Gamma}_\alpha^{\rm expt}$ is estimated to be 6 μeV. We also estimated the average α width from α widths of individual neutron resonances measured in Ref. [15]. From nine 3^- and 4^- resonances with energies up to 705 eV, the estimated average α width turned out to be 5.3 μeV which is in 12% agreement with the value of 6 μeV obtained from the cross-section ratio. The total α width is mainly due to 9.45 MeV α particles populating the ground 0^+ state of the ^{140}Ce nucleus. However, it is important to use the correct energy dependence of $\overline{\Gamma}^{L'}(E_\alpha)$, especially in the energy range E_α from 8 to 9.5 MeV where the $(n,\gamma\alpha)$ cross section is concentrated. For this, we used the experimental cross section of the broad peak located at 7 MeV in the experimental α spectrum (see Fig. 1). This peak includes 10 levels of ^{140}Ce with excitation energies from 2 to 2.6 MeV populated by α particles with energies from 6.8 to 7.2 MeV. Ten levels reduce the Porter–Thomas fluctuations compared to a single-level population. The remaining estimated uncertainty due to these statistical fluctuations is estimated to be about 50%. Transmission coefficients obtained from optical model parameters of Ref. [10] have been scaled to reproduce the average $\Gamma_\alpha^{\rm expt}$ of 6 μeV which is mainly due to 9.45 MeV ground-state transitions. This allows the α-transmission coefficients to be tested for the α energy around $E_\alpha = 7$ MeV to be able to get the correct energy dependence between 7 and 9.45 MeV. Table I presents the experimental α width for the α group 6.8–7.2 MeV as well as widths calculated with different optical potentials from Ref. [10] along with their scaling factors. The best potential has been chosen to be the one from Ref. [16]. In calculations of thermal neutron capture by ^{143}Nd, the value of $\sigma_i = 325$ barns was used as a capture cross section by a 3^- resonance [14] and only (n,γ) and (n,α) outgoing channels were considered.

We tested the following γ-strength-function models. For the $E1$-strength function this is the model developed by Kadmensky–Markushev–Furman (KMF) [4]:

$$f_{E1}^{\rm KMF}(E_\gamma) = \frac{1}{3\pi^2\hbar^2c^2}\frac{0.7\sigma_{E1}\Gamma_{E1}^2\left(E_\gamma^2 + 4\pi T^2\right)}{E_{E1}\left(E_\gamma^2 - E_{E1}^2\right)^2}, \tag{4}$$

where σ_{E1}, Γ_{E1}, and E_{E1} are the giant electric dipole resonance parameters derived from photoabsorption cross sections [21]. The temperature T is usually defined in terms of excitation

TABLE I. Summed α width for transitions with energies 6.8–7.2 MeV populating 10 levels of ^{140}Ce in the excitation energy interval 2 to 2.6 MeV. Widths are calculated with different optical potentials indicated by references. Uncertainties in brackets are expected to be due to Porter–Thomas statistical fluctuations estimated for 10 populated levels.

	Expt.	Calculations					
Reference		[17]	[18]	[19]	[20]	[7]	[16]
Scale factor		0.35	0.08	0.11	4.44	1.7	2.53
Γ_α^5, 10^{-5}	2.9	7.0 (35)	13 (7)	14 (7)	1.1 (6)	1.4 (7)	2 (1)

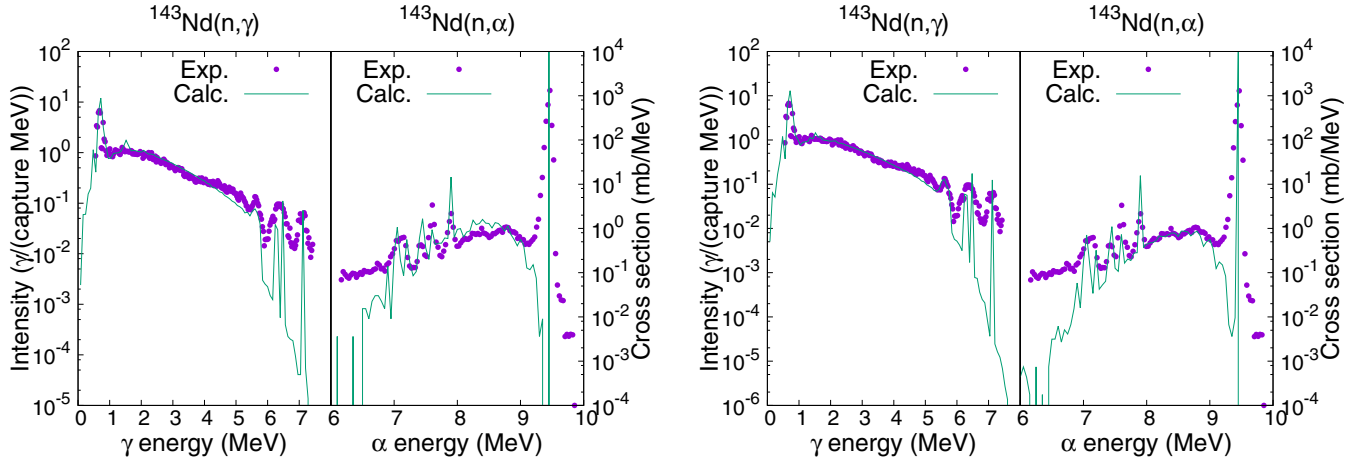

FIG. 2. (Color online) Points are from the experiments for ^{143}Nd$(n,\gamma)^{144}$Nd [25] and ^{143}Nd$(n,\alpha)^{140}$Ce [2] reactions with 15–90 keV and thermal neutrons, respectively. Lines are calculations with the constant-temperature level density model, the KMF $E1$ strength (4) and the SLO (5) for the $M1$-strength function (left panel) and with the constant-temperature level density model, the KMF $E1$ strength (4) and the Weisskopf $M1$ constant strength (right panel).

energy U and the level density parameter a as $\sqrt{U/a}$. Later, the so-called enhanced Lorentzian model was developed and became more popular in interpreting experimental data [5]. However, it does not differ much from the KMF model of Eq. (4). Therefore, since the KMF model was originally used to interpret the ^{143}Nd$(n,\gamma\alpha)$ reaction [3], we use it here as well.

Two $M1$ models have been tested. The first one is the Weisskopf estimate [8] based on the single-particle model which results in the constant strength function $f_{M1}(E_\gamma) =$ const. The value of the constant is estimated from f_{M1}/f_{E1} systematics as prescribed in Refs. [5,10] which recommend this ratio to be $17.2A^{-0.87}$. The second model is based on the assumption of the spin-flip magnetic resonance described by the standard Lorentz (SLO) function as

$$f_{M1}^{\mathrm{SLO}}(E_\gamma) = \frac{1}{3\pi^2\hbar^2c^2}\frac{\sigma_{M1}\Gamma_{M1}^2E_\gamma}{\left(E_\gamma^2 - E_{M1}^2\right)^2 + E_\gamma^2\Gamma_{M1}^2}, \qquad (5)$$

where parameters σ_{M1}, Γ_{M1}, and E_{M1} are taken from Ref. [10].

In calculations of γ cascades in ^{144}Nd, discrete levels were used up to 2.36 MeV. The level density above that energy was modeled with a Fermi gas [22] and the constant-temperature [23] functions. Model parameters were determined from fitting these two functions to the density of discrete levels [24] and to the density of neutron resonances (to the neutron resonance spacing) taken from Ref. [14]. In both cases, the spin cutoff parameter was calculated according to the rigid body model [10] with parameters obtained for the Fermi-gas function. The number of negative and positive levels was assumed to be equal.

Model calculations were tested against both the experimental α spectrum from ^{143}Nd$(n,\gamma\alpha)$ [2] and the experimental γ spectrum from ^{143}Nd(n,γ) reactions [25] measured with thermal and 15–90 keV neutrons, respectively. The comparison is presented in Fig. 2. The best agreement was found with the combination of the constant-temperature model for the level density, the KMF model for the $E1$-strength function and the Weisskopf energy-independent approximation for the $M1$-strength function. However, even in the case of best agreement, there is still a noticeable underestimation of experimental (n,γ) data points by calculations in the region of the high-energy ($E_\gamma > 3.8$ MeV) γ transitions. Since this underestimation also applies to the high-energy peaks related to individual γ transitions, it may be concluded that it is caused by the underestimation of the γ-strength function (rather than by level density) in the high-energy region.

In order to estimate the correct $E1$- and $M1$-strength functions as well as their possible uncertainties which are due to restricted experimental information and uncertainties of experimental data points, the artificial analytical highly parametrized formulas were constructed in the following way: For the $E1$-strength function it is expressed as

$$f_{E1}(E_\gamma) = f_{E1}^{\mathrm{KMF}}(E_\gamma)\left\{\sigma_1\left[\mathrm{erf}\left(\frac{E_\gamma - E_{\mathrm{cut}}}{\Gamma_1}\right) + 1\right] + 1\right\}. \qquad (6)$$

The erf() function allows for the step-like increase of the KMF γ-strength function for $E_\gamma > E_{\mathrm{cut}}$ with a magnitude determined by the parameter σ_1. Here, we made the temperature T constant but it is allowed to vary freely as an adjustable parameter. Zero T makes Eq. (4) approach zero similar to the SLO model (5) such that $f_{E1}^{\mathrm{KMF}}(E_\gamma)_{E_\gamma\to 0} \to 0$. The positive T increases the low-energy $E1$ strength such that it approaches the constant limit $f_{E1}^{\mathrm{KMF}}(E_\gamma)_{E_\gamma\to 0} \to$ const. where the constant value is determined by the parameter T.

The $M1$ γ-strength function was modeled by the equation

$$f_{M1}(E_\gamma) = f_{M1}^{\mathrm{SLO}} + f_{\mathrm{pole}}(E_\gamma), \qquad (7)$$

where $f_{\mathrm{pole}}(E_\gamma) = \sigma_p \exp(-\Gamma_p E_\gamma)$ models the low-energy increase of the $M1$ γ-strength function with parameters σ_p and Γ_p. The $E2$ strength function was approximated by the SLO function with parameters from Ref. [10]. The parameters of both Eqs. (6) and (7) were varied randomly in the following ranges: $T = 0.1$ to 3 MeV, $\sigma_1 = 0$ to 1 mb, $E_{\mathrm{cut}} = 4$ to 5 MeV, $\Gamma_1 = 0.6$ MeV, $\sigma_{\mathrm{p}} = 0.01$ to 1 mb, $\Gamma_p =$ 0 to 2 MeV, resulting in random $E1$ and $M1$ γ-strength functions. For each set of parameters both the (n,γ) and $(n,\gamma\alpha)$

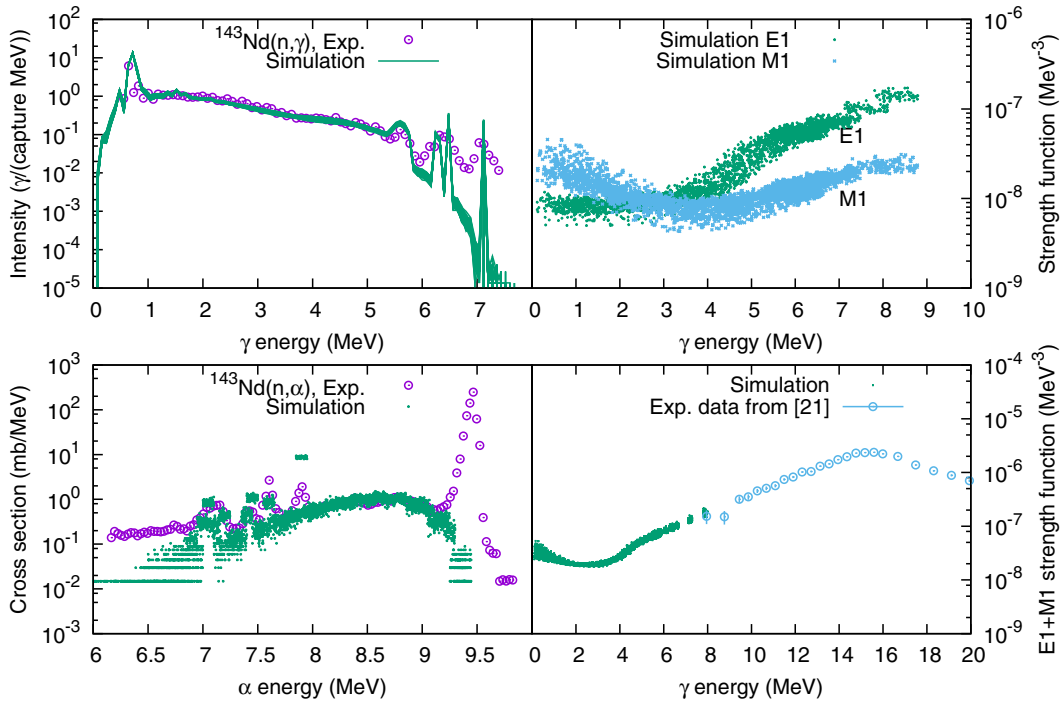

FIG. 3. (Color online) Experimental data as in Fig. 2 (left panel). Scattered points are the result of simulations (see text for explanations). Simulated points corresponding to the population of the ground state in the ^{143}Nd(n,α) ^{140}Ce reaction are up off the scale and not visible in the lower-left plot. Open circles in the lower-right plot are from the photoabsorbtion experiments of Ref. [21].

spectra were calculated and compared with experimental data points. Only those were selected which deviate from experimental points by no more than 15%. It resulted in squeezing the range of the following parameters: $\sigma_1 = 0.2$ to 1 mb, $\sigma_p = 0.1$ to 0.5 mb, and $\Gamma_p = 0.2$ to 1 MeV. Other parameters were allowed within initially assumed ranges.

Both the constant-temperature and the Fermi-gas level density models were tested. It was found that the constant-temperature model allowed reproducing both sets of experimental data within 15% uncertainties, while the Fermi-gas model failed to do that.

Figure 3 presents experimental against simulated spectra along with corresponding $E1$- and $M1$-strength functions. The $E1$ one exhibits a nonzero limit at $E_\gamma \to 0$ which is consistent with the KMF prediction of Eq. (4). The high-energy part is little enhanced to be able to describe the high-energy region of the (n,γ) spectrum. The $M1$ functions are enhanced in the low-energy region compared to the prediction based on the Lorentz function (5). This is in contradiction with conclusions derived from analysis of γ spectra from neutron capture reactions in this mass region [5]. However, it supports results of the analysis of experimental two-step cascade spectra [26] from the ^{143}Nd$(n,2\gamma)$ reaction on thermal neutrons where the best agreement was obtained with the energy-independent Weisskopf model [8] for the $M1$-strength function. This model was also found best to describe the shape of the ^{143}Nd$(n,\gamma\alpha)$ spectrum in the original work of Ref. [3].

Figure 3 shows the sum of $(E1 + M1)$-strength functions in comparison with the strength function obtained from cross-section data of the ^{143}Nd(γ,n) reaction [21] in the region of the giant dipole resonance ($E_\gamma > \sim 8$ MeV). Despite the fact that these two data sets have been obtained with different techniques from different experiments, they show a good agreement at the matching point of about 8 MeV. This supports reliability of both sets of data.

III. SUMMARY

Analysis of both $E1$ and $M1$ γ-strength functions in ^{144}Nd has been performed using available experimental data from ^{143}Nd(n,γ) ^{144}Nd and ^{143}Nd$(n,\gamma\alpha)$ ^{140}Ce reactions. The $E1$ strength was confirmed to have a nonzero limit at γ energy approaching zero $f_{E1}(E_\gamma)_{E_\gamma \to 0} = \text{const}$. This is consistent with the KMF model of Ref. [4] and with conclusions of the original works of Refs. [3,9]. However, for γ energies greater than 3.5 MeV the step-like enhancement is needed to reproduce the high-energy portion of the (n,γ) spectrum from Ref. [25]. The $M1$ strength was found to be comparable with $E1$ strength in the region of low-energy γ transitions (<3 MeV) which implies either low-energy enhancement of the SLO model (5) or the validity of the energy-independent Weisskopf single-particle model [8]. This finding is not consistent with the commonly adopted SLO model for $M1$ strength [10] but it is in accord with the original work of Ref. [3] and with the $M1$ hypothesis of the low-energy enhancement seen in Oslo-type experiments [11].

ACKNOWLEDGMENT

This work was funded by DOE, Grants No. DE-FG02-88ER40387, No. DE-NA0001837, and No. DE-NA0002905.

[1] N. S. Oakey and R. D. Macfarlane, Phys. Lett. B **26**, 662 (1968).
[2] L. Aldea, B. Kardon, O. W. B. Schult, H. Seyfarth, and N. Wüst, Z. Phys. A: At. Nucl. (1975) **283**, 391 (1977).
[3] Yu. P. Popov, Sov. J. Part. Nucl. **13**, 483 (1982).
[4] S. Kadmensky, V. Markushev, and V. Furman, Sov. J. Nucl. Phys. **37**, 165 (1983).
[5] J. Kopecky and M. Uhl, Phys. Rev. C **41**, 1941 (1990).
[6] M. Herman, R. Capote, B. Carlson, P. Obložinský, M. Sin, A. Trkov, H. Wienke, and V. Zerkin, Nucl. Data Sheets **108**, 2655 (2007).
[7] A. J. Koning, S. Hilaire, and M. C. Duijvestijn, in *Proceedings of the International Conference on Nuclear Data for Science and Technology, April 22–27, 2007, Nice, France*, edited by O. Bersillon, F. Gunsing, E. Bauge, R. Jacqmin, and S. Leray (EDP Sciences, Les Ulis, France, 2008), p. 211.
[8] J. M. Blatt and V. F. Weisskopf, *Theoretical Nuclear Physics* (Willey, New York, 1952).
[9] V. K. Thanh, V. A. Vtyurin, and Yu. P. Popov, Inst. Phys. Conf. Ser. **6**, 431 (1982).
[10] R. Capote, M. Herman, P. Obložinský, P. G. Young, S. Goriely, T. Belgya, A. V. Ignatyuk, A. J. Koning, S. Hilaire, V. A. Plujko, M. Avrigeanu, O. Bersillon, M. B. Chadwick, T. Fukahori, Z. Ge, Y. Han, S. Kailas, J. Kopecky, V. M. Maslov, G. Reffo, M. Sin, E. S. Soukhovitskii, and P. Talou, Nucl. Data Sheets **110**, 3107 (2009).
[11] R. Schwengner, S. Frauendorf, and A. C. Larsen, Phys. Rev. Lett. **111**, 232504 (2013).
[12] P. E. Koehler, Y. M. Gledenov, J. Andrzejewski, K. H. Guber, S. Ramas, and T. Rauscher, Nucl. Phys. A **688**, 86c (2001).
[13] K. Wisshak, F. Voss, F. Käppeler, L. Kazakov, and G. Reffo, Phys. Rev. C **57**, 391 (1998).
[14] S. F. Mughabghab, *Atlas of Neutron Resonances* (Elsevier, Amsterdam, 2006).
[15] J. Kvitek and Yu. P. Popov, Nucl. Phys. A **154**, 177 (1970).
[16] V. Avrigeanu, M. Avrigeanu, and C. Manailescu, Phys. Rev. C **90**, 044612 (2014).
[17] L. McFadden and G. R. Satchler, Nucl. Phys. **84**, 177 (1966).
[18] J. R. Huizenga and G. Igo, Nucl. Phys. **29**, 462 (1962).
[19] V. Avrigeanu, P. E. Hodgson, and M. Avrigeanu, Phys. Rev. C **49**, 2136 (1994).
[20] M. Avrigeanu, A. C. Obreja, F. L. Roman, V. Avrigeanu, and W. von Oertzen, At. Data Nucl. Data Tables **95**, 501 (2009).
[21] P. Carlos, H. Beil, R. Bergere, A. Lepretre, and A. Veyssiere, Nucl. Phys. A **172**, 437 (1971).
[22] H. A. Bethe, Phys. Rev. **50**, 332 (1936).
[23] A. Gilbert, F. S. Chen, and A. G. W. Cameron, Can. J. Phys. **43**, 1248 (1965).
[24] "ENSDF data base", http://nndc.bnl.gov/ensdf/, accessed 2015-07-01.
[25] T. Veerapaspong, M. Igashira, S. Mizuno, J. ichi Hori, and T. Ohsaki, J. Nucl. Sci. Technol. (Abingdon, U. K.) **36**, 855 (1999).
[26] F. Bečvář, P. Cejnar, R. E. Chrien, and J. Kopecký, Phys. Rev. C **46**, 1276 (1992).